



香港城市大學  
City University of Hong Kong

專業 創新 胸懷全球  
Professional · Creative  
For The World

## CityU Scholars

### Optimization of Solar-Assisted CCHP Systems

### Enhancing Efficiency and Reducing Emissions Through Harris Hawks-Based Mathematical Modeling

Ukaegbu, Uchechi; Tartibu, Lagouge; Lim, C. W.

#### Published in:

Sustainability (Switzerland)

Published: 01/12/2024

#### Document Version:

Final Published version, also known as Publisher's PDF, Publisher's Final version or Version of Record

#### License:

CC BY

#### Publication record in CityU Scholars:

[Go to record](#)

#### Published version (DOI):

[10.3390/su162310694](https://doi.org/10.3390/su162310694)

#### Publication details:

Ukaegbu, U., Tartibu, L., & Lim, C. W. (2024). Optimization of Solar-Assisted CCHP Systems: Enhancing Efficiency and Reducing Emissions Through Harris Hawks-Based Mathematical Modeling. *Sustainability (Switzerland)*, 16(23), Article 10694. <https://doi.org/10.3390/su162310694>

#### Citing this paper

Please note that where the full-text provided on CityU Scholars is the Post-print version (also known as Accepted Author Manuscript, Peer-reviewed or Author Final version), it may differ from the Final Published version. When citing, ensure that you check and use the publisher's definitive version for pagination and other details.

#### General rights

Copyright for the publications made accessible via the CityU Scholars portal is retained by the author(s) and/or other copyright owners and it is a condition of accessing these publications that users recognise and abide by the legal requirements associated with these rights. Users may not further distribute the material or use it for any profit-making activity or commercial gain.

#### Publisher permission

Permission for previously published items are in accordance with publisher's copyright policies sourced from the SHERPA RoMEO database. Links to full text versions (either Published or Post-print) are only available if corresponding publishers allow open access.

#### Take down policy

Contact [lbscholars@cityu.edu.hk](mailto:lbscholars@cityu.edu.hk) if you believe that this document breaches copyright and provide us with details. We will remove access to the work immediately and investigate your claim.

## Article

# Optimization of Solar-Assisted CCHP Systems: Enhancing Efficiency and Reducing Emissions Through Harris Hawks-Based Mathematical Modeling

Uchechi Ukaegbu <sup>1</sup>, Lagouge Tartibu <sup>1,\*</sup> and C. W. Lim <sup>1,2</sup>

<sup>1</sup> Department of Mechanical Engineering, Faculty of Engineering and the Built Environment, University of Johannesburg, Johannesburg P.O. Box 2028, South Africa; ukaegbuuchechi531@gmail.com (U.U.); bccwlim@cityu.edu.hk (C.W.L.)

<sup>2</sup> Department of Architecture and Civil Engineering, City University of Hong Kong, Hong Kong, China

\* Correspondence: ltartibu@uj.ac.za

**Abstract:** The increasing demand for energy, driven by technological advances, population growth, and economic expansion, has intensified the focus on efficient energy management. Tri-generation systems, such as Combined Cooling, Heating, and Power (CCHP) systems, are of particular interest due to their efficiency and sustainability. Integrating renewable energy sources like solar power with traditional fossil fuels further optimizes CCHP systems. This study presents a novel method for enhancing the CCHP system efficiency by identifying the optimal design parameters and assisting decision makers in selecting the best geometric configurations. A mathematical programming model using the Harris Hawks optimizer was developed to maximize the net power and exergy efficiency while minimizing CO<sub>2</sub> emissions in a solar-assisted CCHP system. The optimization resulted in 100 Pareto optimal solutions, offering various choices for performance improvement. This method achieved a higher net power output, satisfactory exergy efficiency, and lower CO<sub>2</sub> emissions compared to similar studies. The study shows that the maximum net power and exergy efficiency, with reduced CO<sub>2</sub> emissions, can be achieved with a system having a low compression ratio and low combustion chamber inlet temperature. The proposed approach surpassed the response surface method, achieving at least a 4.2% reduction in CO<sub>2</sub> emissions and improved exergy values.

**Keywords:** CCHP; CO<sub>2</sub> emissions; exergy efficiency; net power; tri-generation system; solar energy



check for updates

**Citation:** Ukaegbu, U.; Tartibu, L.; Lim, C.W. Optimization of Solar-Assisted CCHP Systems: Enhancing Efficiency and Reducing Emissions Through Harris Hawks-Based Mathematical Modeling. *Sustainability* **2024**, *16*, 10694. <https://doi.org/10.3390/su162310694>

Academic Editors: Giampaolo Manfrida, Firoz Alam, Cristina Rodriguez and Li Sun

Received: 27 August 2024

Revised: 30 October 2024

Accepted: 30 November 2024

Published: 6 December 2024



**Copyright:** © 2024 by the authors. Licensee MDPI, Basel, Switzerland. This article is an open access article distributed under the terms and conditions of the Creative Commons Attribution (CC BY) license (<https://creativecommons.org/licenses/by/4.0/>).

## 1. Introduction

Energy is a fundamental factor in attaining the economic, social, and environmental growth of any country. A survey by Ramachandran, Mourad and Hamed [1] revealed that the rise in energy consumption in recent times, typically instilled by economic development and population growth, has exacerbated the emission of GHGs, especially CO<sub>2</sub>. This emission poses serious environmental and public health risks, contributing significantly to climate change. The environmental degradation resulting from greenhouse gas emissions from power plants poses a substantial hazard to society due to the effects of global warming. As reported by the International Energy Agency (IEA) [2], global CO<sub>2</sub> emissions have increased by 0.9%, reaching an unprecedented high of approximately 36.8 Gigatons. Hence, it is crucial to employ fundamental techniques geared towards improving the design of power generation systems to increase their efficiency and reduce the pollution of the environment.

Multi-generation systems are born out of the need for more sustainable generation of one or more forms of energy as the output. They are mainly categorized, according to the number of outputs, into co-generation and tri-generation systems. Co-generation, or a combined heat and power system, involves the use of a power-generating unit to produce both power and thermal energy simultaneously. In the conventional separate

power generation systems, the heat energy would have been dissipated immediately to the atmosphere but is recovered in CHP systems to provide heating power thus enabling savings in fuel and GHG emission reduction [3]. Irrespective of the fact that CHP systems have glaring advantages over conventional separate heat and power generation systems, they are susceptible to fluctuations in their system's overall efficiency, especially during the summer seasons when the heating loads are at a minimum [4]. A stable and constant power and thermal energy demand profile is essential to achieve the maximum overall system efficiency all year round. Therefore, it is ideal to incorporate cooling systems into a CHP system to boost its efficiency, hence the concept of CCHP systems.

Tri-generation systems, often referred to as CCHP systems, are an expansion of CHP systems in which a single energy source is used to create electricity, cooling, and heating power. It typically comprises a power generation unit/prime mover, cooling system, and heat recovery systems [5]. The prime mover generates mechanical power which is used to rotate the shaft of an electric motor for the generation of electricity. The thermal energy generated during power generation is utilized to operate heating and cooling systems, such as the absorption chiller and heat recovery generation unit, or to generate more power through the organic Rankine or Kalina cycle.

Renewable sources, especially solar thermal technologies, have been extensively researched as visible solar harvesting options for power generation in a bid to reduce the fossil fuel consumption. Solar thermal collectors are predominantly employed to operate side-by-side with fossil fuels because of their relatively lower cost and higher conversion efficiency when compared to solar photovoltaic technologies [6]. Solar-assisted CCHP systems offer a sustainable approach to energy production by reducing the carbon emissions and operational costs, while also enhancing the system's overall energy efficiency. These systems ensure the reliability and availability of various energy sources [7]. However, its performance can be further improved through optimization, and hence the search for even better thermodynamic performance metrics is underway.

The optimization domain has applied several use cases in solving the challenge associated with the rapid advancement in industrial technology [8]. According to Hansen, Muller, and Koumoutsakos [9], there are generally two types of optimizations: deterministic and metaheuristic algorithms. In the deterministic/heuristic approach, the gradient of the objective function is required, and a constant output is obtained for a given input. The metaheuristic, on the other hand, can solve several types of optimization problems by tuning its parameters, and it does not yield a constant output for a given input. Two common types of metaheuristic optimization are the evolutionary and swarm optimization techniques [10]. The evolutionary algorithm is driven by the principles of mutation, crossover, and survival of the fittest, as proposed by Charles Darwin. On the other hand, the swarm algorithm aims to mimic the foraging behavior of a specific group of animals in order to achieve a certain objective. The genetic algorithm, genetic programming, and differential evolution are valid examples of evolutionary algorithms, and these are presented in Figure 1. Prominent examples of swarm-intelligence algorithms are the Harris Hawks, grey wolf, moth flame, ant colony, ant–lion optimization, etc.

Typically, practical engineering scenarios involve many objectives that often conflict with each other, as indicated by [11]. Multi-objective problems can be resolved by either decomposing them into a single-objective function or by calculating the Pareto optimal solutions while maintaining the multi-objective formulation. This research study employed the latter approach. Other research studies have described various optimization methods, including the RSM [12], non-dominated sorting genetic algorithm-II (NSGA-II) [13], particle swarm optimization (PSO) [14], HHO [15], grasshopper optimization (GOA) [16], ant–lion optimization [17], moth flame optimization (MFO) [18], and grey wolf optimization (GWO) [19].

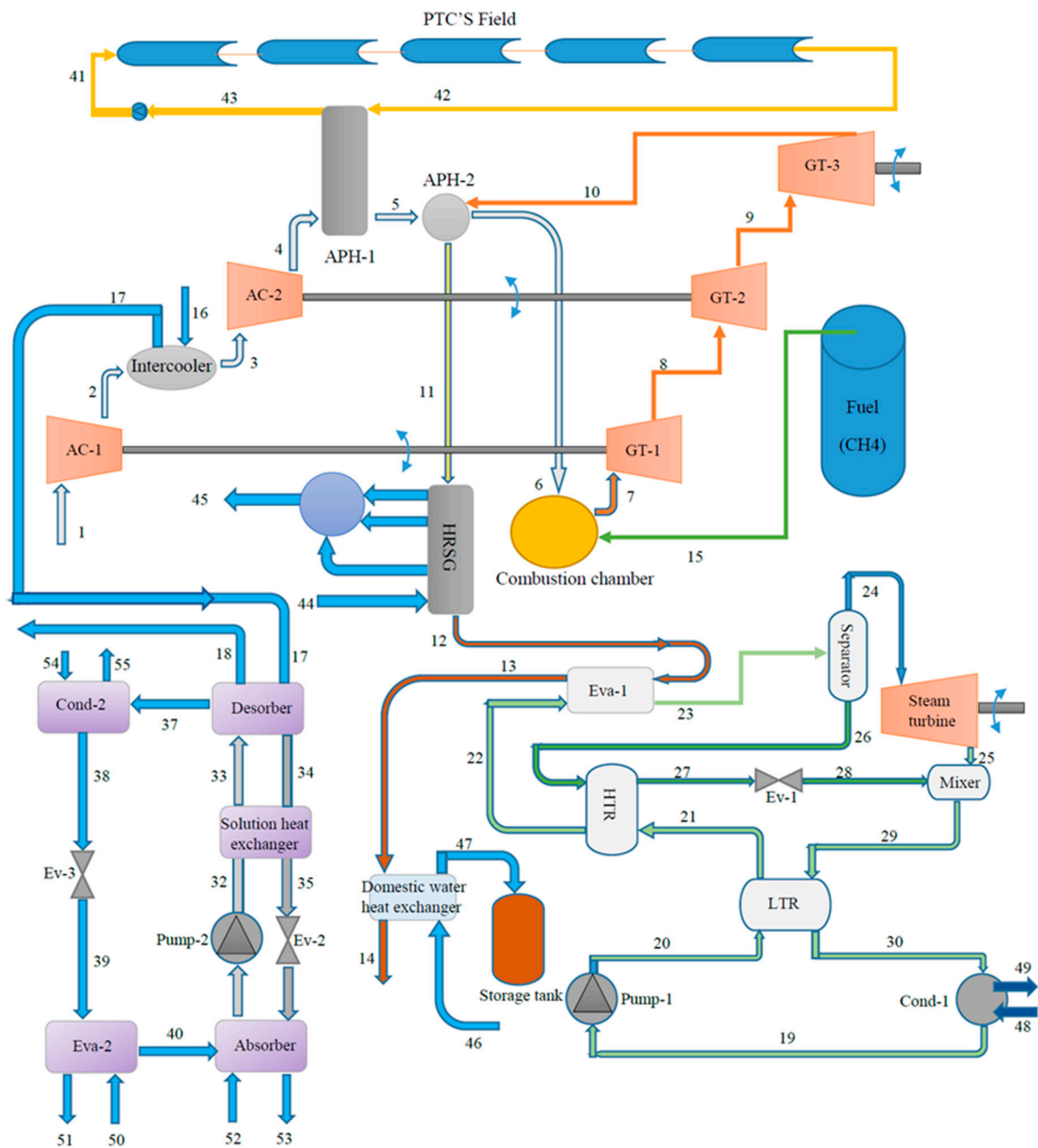


**Figure 1.** An illustration of the solar-assisted CCHP system.

Prior optimization research has shown that the optimization of CCHP systems primarily depends on three key evaluation categories: exergetic, economic, and environmental variables [20]. These criteria form a comprehensive framework for assessing CCHP system optimization and addressing the efficiency, cost-effectiveness, financial feasibility, and environmental impact. Achieving an optimal CCHP system involves balancing these criteria to achieve efficiency, cost-effectiveness, and environmental sustainability. This study demonstrates the application of HHO in formulating and solving a problem associated with a solar-integrated CCHP system. Based on the information provided, the proposed research seeks to achieve the following goals:

- To develop a mathematical model using the Harris Hawks algorithm on a solar-assisted CCHP system.

- Optimize the net power output and exergy efficiency, while simultaneously limiting CO<sub>2</sub> emissions, in a solar energy-integrated CCHP system utilizing the Harris Hawks optimizer.

## 2. Literature Review

The pursuit of continual improvement in CCHP systems through the use of different optimization approaches is a forward-thinking trend in energy conservation and management research. A thorough literature study examines the efforts aimed at optimizing specific performance parameters in solar-based CCHP systems.

A comprehensive examination revealed that a substantial proportion of researchers have employed the genetic algorithm to optimize the CCHP system assisted with solar energy. For example, Cao et al. [21] presented a revised solar-powered CCHP system that utilized the genetic algorithm to enhance the electricity generation, exergy performance, and overall cost per unit exergy. Their parametric study investigated the influence of decision variables, such as the proportion of oil mass, the inlet pressure of the Rankine cycle, and operating temperature, on the performance metrics. This technique exhibited enhanced results across several performance metrics, surpassing the conventional methodologies.

Wang et al. [22] performed a thermodynamic assessment and efficiency improvement of a CCHP system that integrates solar and natural gas. They utilized a genetic optimization technique to maximize the system's energetic and exergetic capacities. Furthermore, Wang et al. [23] devised a multi-objective optimization model that utilizes the genetic algorithm to improve the energy and cost efficiency, reduce CO<sub>2</sub> emissions, and boost the grid integration of the CCHP system. Although their suggested operational flexibility strategy enhanced the ability to respond to changing situations, it resulted in decreased levels of grid contact, as well as reduced exergetic efficiency, cost-effectiveness, and environmental impacts.

Song, Liu, and Lin [24] utilized the NSGA-II algorithm to conduct the multi-objective optimization of a solar-powered CCHP system across three different operational configurations. The decision variables considered were the capacity of the gas turbine, the area of the photovoltaic (PV) system, and the size of the solar collector. The objective was to optimize the ratio of cost saving and energy saving. The findings highlighted the significant impact of energy costs and the performance of the PV panels, solar collectors, and gas turbines on the CCHP system.

The multi-objective Harris Hawks method has been utilized to optimize a variety of multi-generation systems. Abba et al. [25] suggested a hybrid optimization strategy that used Harris Hawks and particle swarm optimization, along with support vector regression (SVR), to estimate the load requirements and optimize the sizing of a hybrid renewable energy system, with the goal of minimizing the annual cost. The findings demonstrated that the suggested HHO-based optimization technique surpassed the single SVR in regard to several performance indicators, such as the coefficient of correlation, coefficient of determination, mean squared error, and root mean squared error.

Yousri, Babu, and Fathy [26] introduced the Harmony Search algorithm as a means to optimize the parameters of a proportional-integral controller within a renewable energy-based system. The optimization of the system focuses on minimizing the integral time absolute error and maximizing the tie-line power. The system includes thermal plants, photovoltaic plants, wind turbines, and other components. The resulting results were validated using the grey wolf optimizer, multi-verse optimizer, and sine cosine algorithm.

Zhao et al. [27] described the enhancement of a fuel cell-based CCHP system by optimizing the use of HHO (hydrogen and oxygen) with the introduction of the singer mechanism. The CCHP system was optimized to maximize the exergy performance, system performance, greenhouse gas reduction, and cost efficiency. The computed results were assessed using both the conventional HHO and the NSGA-II algorithms. The updated HHO approach exhibited a reduced exergy efficiency and increased greenhouse gas reduction.

Song, Tan, and Mizzi [28] introduced an adapted HHO method to optimize a proton exchange membrane fuel cell. The HHO method underwent modifications by incorporating

the quasi-oppositional concept and a logistic map mechanism. These modifications were aimed at enhancing the system's speed and robustness. This approach was implemented in three case studies and assessed by comparing it with the krill herd method, grass fibrous root optimization, and a conventional HHO algorithm. The objective of reducing the squared deviation between the output voltage and predicted data was successfully accomplished as the proposed approach yielded satisfactory outcomes.

In addition, Pandey and Jadoun [29] investigated the optimal scheduling strategies for a virtual power plant consisting of photovoltaic solar collectors, a wind energy source, a fuel cell, and a CCHP system. A modified HHO system was used to reduce both the financial gains and emissions. The optimization technique was enhanced by augmenting the step duration of the Hawks and incorporating a chaotic mapping mechanism to amplify the algorithm's diversity. The acquired solutions were verified using data from the particle swarm optimization (PSO) and mixed linear programming.

Mahalekshmi and Maruthupandi [30] utilized the Harmony Search algorithm to address the issues of economic and emission dispatch in power systems. The proposed method utilized a fuzzy-based technique to control the size of the Pareto optimal solutions. The overall system was then optimized for emission dispatch and total cost. The acquired findings were evaluated for quality using set spacing, hyper volume, and CM, and were compared with the results derived from the PSO technique.

Mahdavi, Mojaver, and Khalilarya [31] developed an innovative solar-powered CCHP system. The researchers utilized the RSM to perform multi-objective optimization, specifically targeting the net power output, CO<sub>2</sub> emission reduction, and exergy efficiency. In this system, the waste heat generated between the compression stages is captured via a cooling unit to drive a chiller system. By analyzing the combined impacts of several key parameters, a set of six optimal configurations were identified. The TOPSIS approach was utilized to determine the most favorable solution, yielding ideal outcomes for the net power output, CO<sub>2</sub> emission reduction, and exergy efficiency, respectively.

This section has examined literary works, summarized in Table 1, that have showcased the efficacy of solar-integrated CCHP systems. Furthermore, this literature analysis emphasized the increasing enthusiasm for utilizing these optimization techniques in multi-generation systems, such as the CCHP. Furthermore, the author found no evidence of the HHO being utilized in a solar-assisted CCHP system, to the best of their knowledge. Also, related studies have produced relatively high CO<sub>2</sub> emission rates, hence the need for improvement. Given this, this study proposes a new approach based on the HHO. Therefore, the objective of this research was to utilize the HHO to optimize a solar-assisted CCHP system, based on the insights gained from previous studies.

**Table 1.** Overview of relevant studies.

S/N	Source	Methods for Optimization	Renewable Energy Employed	Metrics for Performance Improvement	System Analyzed
1	Cao et al. [21]	Genetic algorithm	Solar	Exergy efficiency, net output electricity and cost per unit exergy	Tri-generation
2	Wang et al. [22]	Genetic algorithm	Solar, natural gas	Energy efficiency, exergy efficiency	Tri-generation
3	Wang et al. [23]	Genetic algorithm	Solar	Primary energy saving ratio, CO <sub>2</sub> emission reduction ratio, annual cost saving rate	Tri-generation
4	Song Liu and Lin [24]	NSGA-II	Solar	Annual cost saving ratio, primary energy saving ratio	Tri-generation
5	Abba et al. [25]	HHO, PSO & SVR	Solar	Annual capital and maintenance cost	Power generation

Table 1. Cont.

S/N	Source	Methods for Optimization	Renewable Energy Employed	Metrics for Performance Improvement	System Analyzed
6	Yousri, Babu, and Fathy [26]	HHO	Solar, wind	Integral time absolute error, tie-line power	Power generation
7	Zhao et al. [27]	HHO	N/A	GHG emission reduction, exergy efficiency, annual cost rate	Tri-generation
8	Song, Tan, and Mizzi [28]	HHO	N/A	Squared deviation between the actual and true output voltage	Power generation
9	Pandey and Jadoun [29]	HHO	N/A	Net profit, GHG emission reduction	Co-generation
10	Mahalekshmi and Maruthupandi [30]	HHO	Wind	Total cost, emission dispatch	Power generation

### 3. Materials and Methods

#### 3.1. Description of the System

This study specifically examines the solar-assisted CCHP system described in the research conducted by Mahdavi et al. [31]. The system depicted in Figure 1 comprises three gas turbines, two compressors, a Kalina cycle, an absorption chiller, solar collectors, an HRSG, and a hot water generator.

The system presented functions using a specific sequence that includes multiple components. The air, at 298.15 K and 1.013 bar, is compressed using two-stage compressors with a cooling unit positioned between them. The waste heat generated by the cooling unit is utilized to power an absorption chiller, which aids in the heat transfer process within a desorber. Afterward, the warmed air, which has been heated by both solar energy and the exhaust gases from a gas turbine in air preheaters up to a temperature of 850 K, combines with methane fuel injected at a temperature and pressure of 298.15 K and 12 bar into the combustion chamber to produce high-temperature gases up to 1520 K. These gases are utilized to operate three gas turbines, with the third turbine being responsible for driving a generator that produces electrical power. In addition, the waste gases from the third gas turbine are used to heat the HRSG, the Kalina cycle via an evaporator (Eva-1), and a household water heat exchanger before being discharged into the ambient surroundings.

In the Kalina cycle, a mixture of ammonia and water, in a saturated liquid state, is pumped to increase its pressure. It then flows through two heat exchangers, namely the low-temperature recuperator and the high-temperature recuperator, to increase its heat content. This process helps to reduce the amount of energy needed for Eva-1. The resultant mixture is divided into saturated vapor and liquid states, with the vapor utilized to provide the work output in a steam turbine. Simultaneously, the fully saturated liquid is sent back to the HTR in order to recover heat energy, prior to being directed through Expansion Valve-1 (Ev-1), which reduces its pressure. Afterwards, the low-pressure saturated liquid at a temperature of 375 K is mixed with the steam turbine output that comprises the liquid-vapor states. The mixture is then transported through the LTR to disperse its energy before being expelled into the environment in a liquid state at a temperature of 303.15 K through Condenser-1 (cond-1), thus concluding the cycle.

The single-effect absorption chiller utilizes a series of operations to extract energy at the desorber by utilizing the discarded gases from the intercooler. The obtained energy is subsequently used to generate a cooling load at the corresponding evaporator (Eva-2). Pump-2 is applied to the weak LiBr-H<sub>2</sub>O solution which then absorbs thermal energy from the rich LiBr-H<sub>2</sub>O working fluid contained in the desorber at state 34. The working fluid, in a gaseous state, flows from the desorber into the condenser (cond-2) after coming into contact with the subcooled liquid from Eva-2 (state 40). In cond-2, the vapor undergoes

condensation and transforms into a saturated liquid. Afterwards, it flows via the expansion valve (Ev-3) and enters Eva-2 where sub-cooling occurs. In Eva-2, the saturated liquid is transformed to cooled saturated vapor which is absorbed (state 40) by the rich LiBr-H<sub>2</sub>O solution thus reverting to its original saturated liquid state at the start of the cycle. States 50 to 51 indicate the cooled water stream provided by Eva-2 which is also utilized in the absorber (52 to 53) to reduce the temperature of the rich LiBr-H<sub>2</sub>O. The water stream with an increased temperature (after coming into contact with the rich LiBr-H<sub>2</sub>O) is used in states 53 to 54 to condense the incoming water vapor from state 37.

The system's operation was based on several assumptions, including constant operating conditions, minimal fluctuations in the kinetic and potential energy, and insignificant thermal losses from the components other than the combustion chamber. The arrows used in Figure 1 indicate the direction of the flow of the combustion fluids.

### 3.2. Response Surface Method

The RSM is an analytical approach used to optimize and model complex systems by examining the relationship between the input variables and output results [32]. The RSM involves creating regression models to describe the link between a specific outcome and its influencing factors. The main procedures include the following:

- **Experimental design:** This stage entails establishing the circumstances for the experiment. It involves choosing pertinent input factors that may influence the response variable. Constraints are subsequently identified to evaluate the design variables during the experiment.
- **Experimental testing:** This involves the execution of tests according to a predetermined experimental strategy. Data pertaining to the outcome variable are gathered across different combinations of design factor levels. These tests are carefully performed to minimize the influence of less significant design variables.
- **Regression model fitting:** This involves the development of models utilizing the data collected from experiments. This is accomplished using techniques such as the least squares or maximum likelihood estimation. The resulting regression models are evaluated to determine their level of conformity to the initial model assumptions.
- **Validation of the regression model:** This occurs after successful fitting of the model by predicting the outcomes using new, unused data from further experimental tests. This stage guarantees the dependability and precision of the established model.

Mahdavi, Mojaver, and Khalilarya [31] employed the response surface methodology to develop regression models that can estimate the net power, CO<sub>2</sub> emission, and exergy efficiency of the system presented in Section 3.1. Table 2 and Equations (10)–(12) display the decision variables, constraints, and objectives.

**Table 2.** Decision variables.

Symbol	Decision variable	Constraints
X <sub>1</sub>	Compression ratio	$10 \leq X_1 \leq 15$
X <sub>2</sub>	Pinch point temperature differential	$10 \leq X_2 \leq 30$
X <sub>3</sub>	Turbine inlet temperature	$1420 \leq X_3 \leq 1520$
X <sub>4</sub>	Combustion chamber inlet temperature	$850 \leq X_4 \leq 950$

This study entails the examination of three separate objective functions:

1. **Net power output:** This refers to the combined power created by the gas turbine and the Kalina cycle, taking into account the work generated from both systems. The mathematical expression can be represented using the formula proposed by Mahdavi, Mojaver, and Khalilarya [31].



$$\dot{P}_{net} = \dot{P}_{net, GT} + \dot{P}_{net, KC} \quad (1)$$

$$\dot{P}_{net, GT} = (\dot{P}_{GT-1} + \dot{P}_{GT-2} + \dot{P}_{GT-3}) - (\dot{P}_{AC-1} - \dot{P}_{AC-2}) \quad (2)$$

$$\dot{P}_{net, KC} = \dot{P}_{ST} - \dot{P}_{pump-2} \quad (3)$$

$$\dot{P}_{GT-1} = \dot{m}_p(h_7 - h_8) = \dot{P}_{AC-1} \quad (4)$$

$$\dot{P}_{GT-2} = \dot{m}_p(h_8 - h_9) = \dot{P}_{AC-2} \quad (5)$$

$$\dot{P}_{GT-3} = \dot{m}_p(h_9 - h_{10}) \quad (6)$$

where

$\dot{P}_{net}$  = net power output;

$\dot{P}_{net, GT}, \dot{P}_{net, KC}$  = net power generated by gas turbines and the Kalina cycle respectively;

$\dot{P}_{GT-1}, \dot{P}_{GT-2}, \dot{P}_{GT-3}$  = net power generated by the three gas turbines;

$\dot{P}_{AC-1}, \dot{P}_{AC-2}$  = net power delivered to the two gas turbines;

$\dot{P}_{ST}, \dot{P}_{pump-2}$  = net power generated by the steam turbine and pump2;

$h_7, h_8, h_9, h_{10}$  = specific enthalpies at the respective states;

$\dot{m}_p$  = mass flow rate of the combustion gases exiting the combustion chamber.

2. Exergy efficiency: This is a useful and effective measure used to evaluate the extent, size, and positions of the irreversibilities in a thermodynamic system [33]. The efficiency is mathematically defined as the quotient of the output exergy divided by the input exergy.

$$\varepsilon = \frac{\dot{P}_{net} + (\dot{E}_{45} - \dot{E}_{44}) + (\dot{E}_{50} - \dot{E}_{51}) + (\dot{E}_{47} - \dot{E}_{46})}{\dot{E}_{in}} \quad (7)$$

$$\dot{E}_{in} = \dot{E}_{fuel} + \dot{E}_{coll} \quad (8)$$

where

$\varepsilon$  = Exergy efficiency;

$\dot{E}_{44}, \dot{E}_{45}, \dot{E}_{46}, \dot{E}_{47}, \dot{E}_{50}, \dot{E}_{51}$  = Exergy at state 44, 45, 46, 47, 50, and 51;

$\dot{E}_{in}$  = Input exergy;

$\dot{E}_{fuel}$  = Exergy of fuel;

$\dot{E}_{coll}$  = Exergy of solar collector.

3. CO<sub>2</sub> Emission: The discharge of CO<sub>2</sub> into the atmosphere poses adverse environmental impacts, emphasizing the ongoing need for its mitigation within thermal energy systems. Emission, a metric assessing the level of CO<sub>2</sub> production, is defined as the ratio of the mass flow rate of CO<sub>2</sub> to the overall output energy, as defined by Mahdavi and Khalilarya [31].

$$\text{Emission} = \frac{\dot{m}_{CO_2}}{\dot{P}_{net} + \dot{Q}_{heating} + \dot{Q}_{cooling}} \quad (9)$$

where

$\dot{Q}_{heating}$  and  $\dot{Q}_{cooling}$  = Heating and cooling loads of the CCHP system;

$$\begin{aligned} \dot{P}_{net}(\text{MW}) = & 62.19 + 0.4573.X_1 + 0.0259.X_2 - 0.02421.X_3 + 0.03638.X_4 - 0.010867.X_1.X_1 \\ & - 0.000029.X_2.X_2 + 0.000005.X_3.X_3 - 0.000009.X_4.X_4 - 0.0003.X_1.X_2 + 0.00022.X_1.X_3 \\ & - 0.00042.X_1.X_4 - 0.000005.X_2.X_3 - 0.000005.X_2.X_4 - 0.000003.X_3.X_4; \end{aligned} \quad (10)$$

$$\begin{aligned} \text{Emission} \left( \frac{\text{gr}}{\text{MJ}} \right) &= 13.1 + 3.722.X_1 + 0.2003.X_2 - 0.0122.X_3 + 0.0451.X_4 - 0.03047.X_1.X_1 \\ &+ 0.0000296.X_2.X_2 + 0.00004.X_3.X_3 + 0.000052.X_4.X_4 + 0.0049.X_1.X_2 - 0.00294.X_1.X_3 \\ &+ 0.00286.X_1.X_4 - 0.000285.X_2.X_3 + 0.000285.X_2.X_4 - 0.000099.X_3.X_4; \end{aligned} \quad (11)$$

$$\begin{aligned} \varepsilon(\%) &= -29 - 0.36.X_1 + 0.287.X_2 + 0.0659.X_3 + 0.0133.X_4 - 0.01807.X_1.X_1 - 0.000029.X_2.X_2 \\ &- 0.000011.X_3.X_3 - 0.000009.X_4.X_4 - 0.0125.X_1.X_2 + 0.0003.X_1.X_3 + 0.00086.X_1.X_4 \\ &- 0.000205.X_2.X_3 + 0.000195.X_2.X_4 - 0.000009.X_3.X_4. \end{aligned} \quad (12)$$

### 3.3. Harris Hawks Optimization

This optimization technique is inspired by one of the smartest birds, usually located in South Arizona USA, known as Harris's hawk [34]. These hawks have a peculiar behavior of carrying out coordinated exploration, attacking, and feeding off their prey while in groups. They mainly employ the "surprise pounce" or "seven kills" tactics to catch their prey. This involves a situation where a group of hawks, emerging from different angles, simultaneously converge on the fleeing prey.

The HHO, proposed by Heidari et al. [35], is a common nature-inspired meta-heuristic algorithm that mimics the exploration and attacking behavior of the Harris's hawk. The stages of the HHO in capturing the prey and can be modeled using the following equations.

$$A = 2A_0 \left( 1 - \frac{r}{R} \right) \quad (13)$$

$$A_0 = 2t_1 - 1 \quad (14)$$

where

$A$  = flight energy of the prey;

$r$  = number of initial repetitions;

$R$  = number of maximum repetitions;

$A_0$  = initial flight energy of the prey and is a random number in  $[-1, 1]$ ;

$t_1$  = random value in  $[0, 1]$ .

The value of  $A$  steadily reduces with each iteration since it is correlated with the prey's flight energy. The prey is said to be physically exhausted when  $A_0$  reduces from 0 to  $-1$  and strengthened when  $A_0$  is increased from 0 to 1. Hence, when  $A \geq 1$ , the hawks are still in the process of searching in various areas for the prey's whereabouts, and this is called the exploration phase. This process is transitioned to the exploitation phase when  $A < 1$ , indicating that the hawks are prepared to capture the prey. The subsequent section will provide a more detailed explanation of these stages.

#### 3.3.1. Exploration Stage

This is the first stage of the hunting process whereby the hawks (also known as candidate solutions) monitor, track, and locate prey (also known as the target) using their powerful eyes. If an equal likelihood,  $t$ , for each waiting strategy is considered,  $m < 0.5$  depicts the condition for the first waiting method while  $m \geq 0.5$  depicts the condition for the second waiting method. Both methods are modeled in Equation (15).

$$Y(r+1) = \begin{cases} Y_{rand}(r) - t_2 |Y_{rand}(r) - 2t_3 Y(r)| & m \geq 0.5 \\ (Y_{prey}(r) - Y_n(r)) - t_4(LB + t_5(UB - LB)) & m < 0.5 \end{cases} \quad (15)$$

where

$Y(r+1)$  = new position of the hawks based on  $r$  repetitions;

$Y_{prey}$  = position of the prey;

$Y_n$  = average position of the current hawks' population;

$Y_{rand}(r)$  = arbitrarily chosen hawk from the hawks' population;  
 $Y(r)$  = the present position of the hawk;  
 $t_2, t_3, t_4, t_5, m$  = random values in  $(0, 1)$  updated in each repetition,  $r$ ;  
 $LB$  = lower bound of the variable;  
 $UB$  = upper bound of the variable.

### 3.3.2. Exploitation Stage

This step is known as the “surprise pounce” phase, in which the hawks employ tactical maneuvers to capture the prey that they have spotted after the exploring phase. During the exploitation stage, the HHO models four different methods based on the prey's avoidance behavior and the assault method of the Harris's hawks. These tactics rely on the likelihood of finding the desired solution and the energy of the prey. The options consist of the soft besiege, hard besiege, soft besiege with progressive rapid dives, and hard besiege with progressive rapid dives.

### 3.3.3. Single-Objective Harris Hawks Optimization

Based on the above-mentioned equations, a mathematical model was developed, and it followed the following methodology:

1. Problem definition: the objective functions and the HHO parameters such as upper and lower boundaries of the decision variables, maximum number of iterations, etc. were defined.
2. Initialization: The initial population size of solutions was initialized. The initialization function was created to ensure that the initialized values do not exceed the defined boundaries of the decision variables.
3. Evaluation: The prey's energy, calculated using Equations (13) and (14), determined if the HHO algorithm employed exploration or exploitation. For any of the two methods employed, the prey's energy was employed to calculate the fitness value of the hawks (objective value) while the prey's location was regarded as the solution for the decision variable. The prey's location and hawks' fitness value were updated at each iteration until the maximum number of iterations was attained. The prey's location at the final iteration became the optimal decision variable solution returned by the algorithm and the corresponding objective value was obtained.

### 3.3.4. Multi-Objective Harris Hawks Optimization

The multi-objective Harris Hawks optimization is inspired by the multi-objective grey wolf technique to perform organized hunting by the Harris hawks. The MOHHO utilizes an archive repository and a roulette wheel approach to store non-dominated Pareto solutions in the archive. During each iteration, newly discovered non-dominated solutions are compared with the existing ones before updating the archive. Once the archive reaches its maximum capacity, the most densely populated solutions are discarded to make space for new entries. The likelihood of removing a solution from the archive is governed by:

$$P_i = \frac{N_i}{c}, c > 1 \quad (16)$$

where

$c$  = constant value;

$N_i$  = number of solutions around the  $i$ th solutions.

To develop the mathematical model for the multi-objective HHO, additional components were integrated into the model for single-objective HHO. The model comprised the following:

1. Problem definition: All three objective functions as well as the upper and lower boundaries of the decision variables were defined. Additionally, parameters such as the inertia weight, global learning coefficient, inflation rate, leader selection pressure, mutation rate, etc., were defined.

2. Initialization: the initial population size, number of iterations, and archive/repository size were initialized to store the non-dominated solutions.
3. Iteration improvement: The leader selection approach was employed in this algorithm to maintain the diversity of the repository. The leader selection pressure parameter (beta) and the non-dominated solution were passed as arguments to the “leader” function and yielded the fittest non-dominated solution as the output. This output was subsequently employed to guide the algorithm in performing exploration and exploitation. The roulette wheel was employed to select the leader of the MOHHO where each solution’s probability of being selected as a leader depended on their fitness value.
4. Evaluation: During the evaluation process, the Pareto dominance was used to determine the domination of the solutions. During each iteration, a solution was included in the archive if it outperformed one or more of the existing solutions in the archive and if neither the new solution nor the existing solutions in the archive outperformed each other. However, a recently acquired solution was excluded from the archive if it was surpassed by at least one of the existing solutions. When a solution was added to the archive, a resident solution was deleted to maintain the pre-defined archive size. Within each iteration, non-dominated solutions and objective values were obtained and updated until the maximum m number of iterations was attained. The Pareto fronts were used to represent the optimal solutions and their accompanying objective values.

The developed models were implemented on MATLAB R2023a for single- and multi-objective optimization. Table 3 shows the MOHHO parameters employed. Figures 2 and 3 display the flowcharts for single- and multi-objective optimization using Harris Hawks.

**Table 3.** Hyperparameter values for MOHHO.

S/N	Parameter	Value
1	Maximum Iterations (MaxIt)	100
2	Population Count (nPop)	100
3	Repository Capacity (nRep)	100
4	Inertia Weight	0.5
5	Inertia Weight Damping Factor	0.99
6	Personal Learning Factor	1
7	Global Learning Factor	2
8	Grids per Dimension (nGrid)	4
9	Inflation Factor (alpha)	0.1
10	Leader Selection Pressure (beta)	2
11	Deletion Selection Pressure (gamma)	2
12	Mutation Rate (mu)	0.1

### 3.4. Mathematical Formulation

The mathematical expression for optimizing the net power is as follows:

$$\text{Maximize } \mathcal{F} = \{P_{\text{net}}(X_1, X_2, X_3, X_4)\} \quad (17)$$

Similarly, the process of optimizing CO<sub>2</sub> emission with a single target can be expressed as follows:

$$\text{Maximize } \mathcal{F} = \{-\text{emission}(X_1, X_2, X_3, X_4)\} \quad (18)$$

The single-objective optimization of exergy efficiency can be expressed as follows:

$$\text{Maximize } \mathcal{F} = \{\varepsilon(X_1, X_2, X_3, X_4)\} \quad (19)$$

The multi-objective optimization problem is defined as follows:

$$\text{Maximize } \mathcal{F} = \{P_{\text{net}}(X_1, X_2, X_3, X_4), \varepsilon(X_1, X_2, X_3, X_4), -\text{emission}(X_1, X_2, X_3, X_4)\} \quad (20)$$

Equations (17)–(20) are subject to the constraints stated in Table 2.

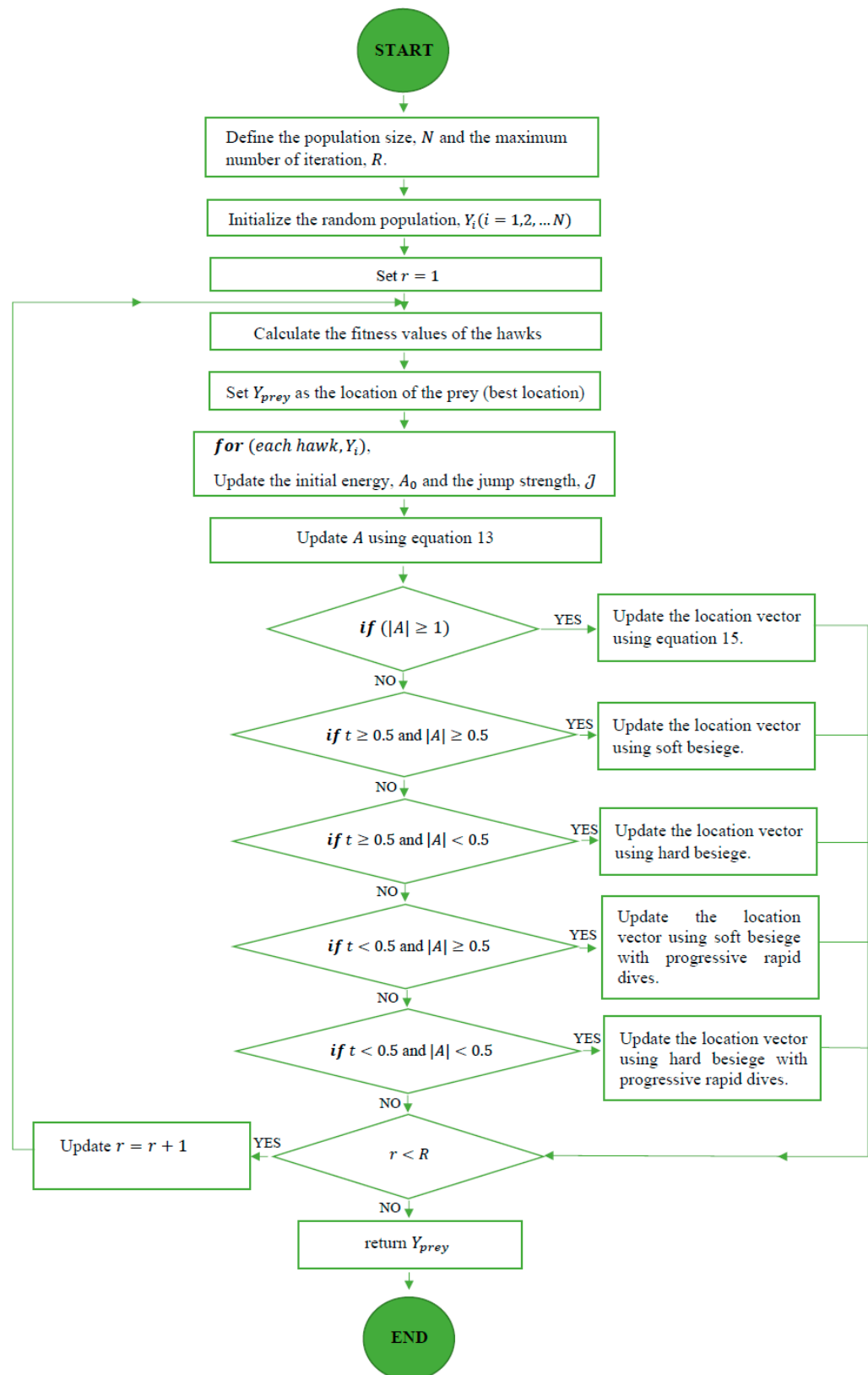


Figure 2. Flowchart for single-objective Harris Hawks optimization.

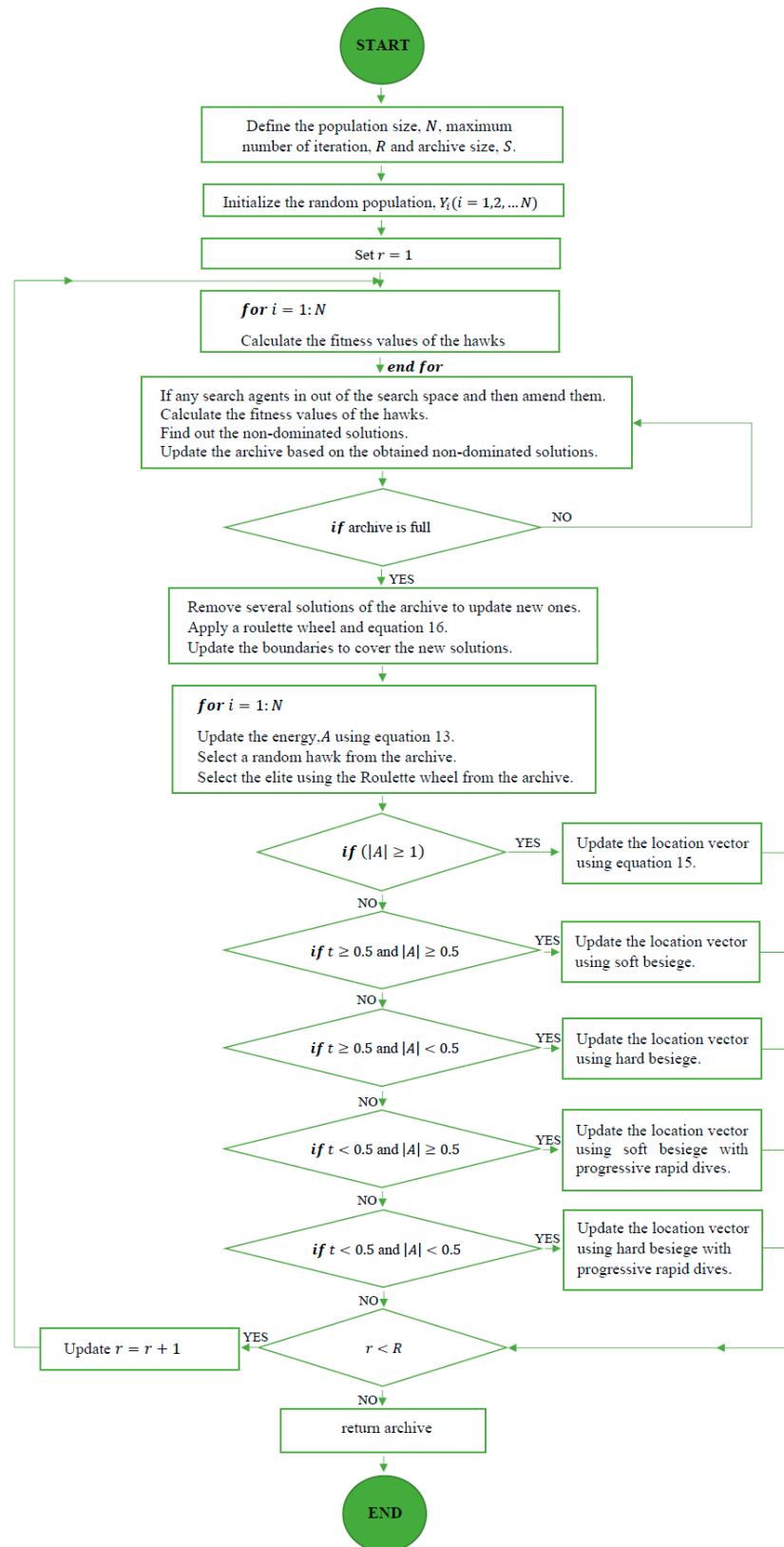


Figure 3. Flowchart for multi-objective Harris Hawks optimization.

## 4. Results and Discussion

### 4.1. Single-Objective Optimization

A single-objective HHO algorithm was executed on each objective function for 100 iterations, employing a search agent population size of 100. The MATLAB codes were run on a laptop that has an Intel Core i3-5005U CPU running at a speed of 2.00 GHz and 8 GB of RAM.

#### 4.1.1. Net Power, CO<sub>2</sub> Emission, Exergy Efficiency, and Optimization

The solutions for Equations (10)–(12) were derived utilizing the decision variables and the respective values listed in Table 2, utilizing the HHO algorithm. The outcomes, shown in Table 4, highlight the necessary steps to enhance the net power and exergy efficiency while simultaneously reducing the CO<sub>2</sub> emissions. The key optimization steps for the net power and CO<sub>2</sub> emission are as follows:

- Lower the compression ratio, pinch point temperature difference, and the combustion chamber inlet temperature.
- Increase the turbine inlet temperature.

**Table 4.** Optimal solutions optimizing the net power, CO<sub>2</sub> emission, and exergy efficiency.

Objective	X <sub>1</sub>	X <sub>2</sub>	X <sub>3</sub>	X <sub>4</sub>	Optimal Objective Value
Maximum Power (MW)	10	10	1520	850	60.8552
Minimum CO <sub>2</sub> (gr/MJ)	10	10	1520	850	49.3771
Maximum Exergy Efficiency (%)	10	10	1420	950	42.3507

To enhance the exergy efficiency, the implementation of the following procedures is necessary:

- Decrease the compression ratio, pinch point temperature difference, and turbine inlet temperature.
- Increase the combustion chamber inlet temperature to its highest possible level.

#### 4.1.2. Analysis of the Single-Objective Optimization Outcomes

The results obtained in Table 4 have been summarized in Table 5, which shows the behavior of the optimal solutions. As shown in Table 5, an upward trend is represented by ↑, a downward trend is represented by ↓, while a conflict between the parameters is indicated by ≠. It could be seen that for decision variables X<sub>1</sub> and X<sub>2</sub>, all three objective functions are in harmony. However, for the X<sub>3</sub> and X<sub>4</sub> decision variables, the exergy efficiency conflicts with the net power and CO<sub>2</sub> emission. Thus, a simultaneous optimization of the three objectives is required to determine the Pareto optimal solutions.

**Table 5.** Illustration of the trend of the objective functions.

Decision Variable	Net Power	CO <sub>2</sub> Emission	Exergy Efficiency
X <sub>1</sub>	↓	↓	↓
X <sub>2</sub>	↓	↓	↓
X <sub>3</sub>	↑	↑	↓≠
X <sub>4</sub>	↓	↓	↑≠

### 4.2. Multi-Objective Optimization

The optimization algorithm has produced a hundred non-dominated solution sets, in the Pareto front as shown in Figure 4. The ensuing optimal solution sets provide the best feasible trade-offs despite the inherent conflicts between the three objectives. Each solution on the Pareto front represents a potential optimal, with the final selection determined by the judgment of the decision-maker.

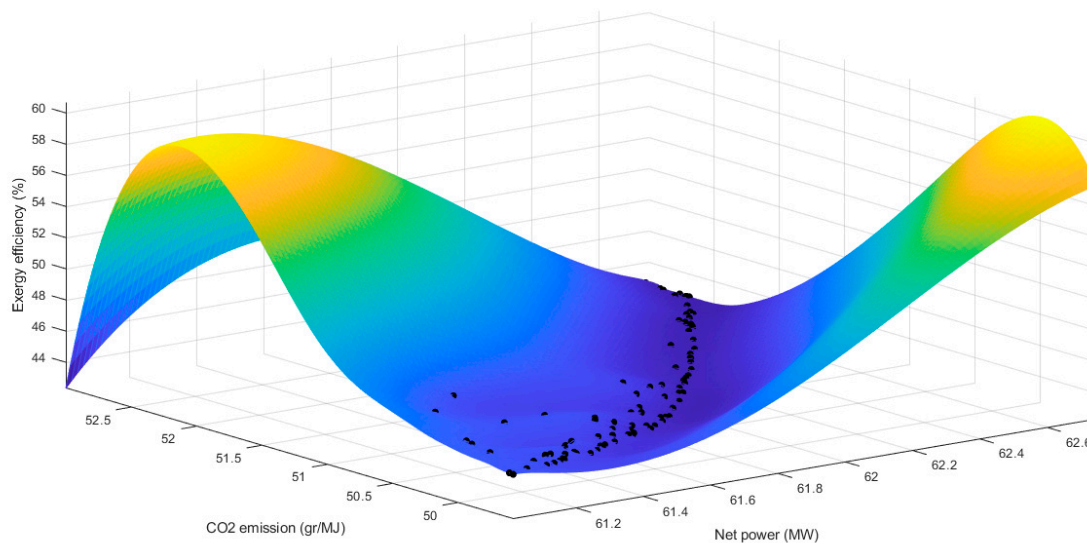


**Figure 4.** Pareto front illustrating the relationship between CO<sub>2</sub> emissions, net power, and exergy efficiency.

An analysis was conducted on three scenarios to have a deeper comprehension of the correlation between each objective function. This study examined the correlations between the CO<sub>2</sub> emissions and net power output, exergy efficiency and net power output, and exergy efficiency and CO<sub>2</sub> emissions in various situations. For clarity, the overall outcomes have been condensed into three two-dimensional Pareto fronts that emphasize crucial aspects. Figure 5 shows the Pareto front, highlighting the trade-off between the net power and CO<sub>2</sub> emissions during the decision-making process as the CO<sub>2</sub> emission rate increased from 50.5 to 51 gr/MJ following an increase in net power from 61.85 to 62.1 MW. This increase is largely due to the higher fuel consumption and intensified combustion processes needed to achieve the additional power output, which naturally leads to more significant carbon emissions. Thus, maximizing the net power will unavoidably result in increasing CO<sub>2</sub> emissions, which may have detrimental consequences for the environment. This emphasizes the need for a balance between maximizing power and minimizing the emissions within the CCHP system. In the CCHP system under study, the net power output was significantly influenced by the power generated by the GT-3 and then the Kalina cycle. To mitigate the CO<sub>2</sub> emissions without substantially compromising the net power output, the system can be configured to ensure that the combustion gases entering from APH-2 reach the unfired HRSG at a higher temperature than when they enter the combustion chamber. Furthermore, it is feasible to simultaneously reduce the rate of fuel consumption and improve the output of the photovoltaic thermal collectors. These adjustments enhance the energy conversion efficiency of the HRSG, resulting in lower fuel use per unit of power generated. The principal power source of the system, the GT-3, produces less net power as a result of these modifications, which are intended to minimize the CO<sub>2</sub> emissions. However, there will be an increase in the cleaner, non-combustible power output from the Kalina cycle. Even if in the end, this method lowers the net power generated, it is optimized to minimize the CO<sub>2</sub> emissions.

Figure 6 demonstrates the relationship between the exergy efficiency and CO<sub>2</sub> emissions as increasing the exergy efficiency value from 42.75 to 44.5 which reduced the CO<sub>2</sub> emissions by about 2.5%, thus indicating a compatibility between the two. An increased exergy efficiency is correlated with a lower CO<sub>2</sub> emission value. This correlation can be attributed to the improved energy conversion processes within the CCHP system, which reduce waste energy and require less fuel input. By achieving a higher exergy efficiency, the system utilizes a greater portion of the available energy, thereby decreasing the CO<sub>2</sub> emissions through lower fuel consumption. This was seen to be in alignment with similar studies that analyzed a double-effect absorption chiller [36] and a solar-assisted energy



storage CCHP system [37]. Figure 6 also shows that in order to significantly boost the energy efficiency, the CO<sub>2</sub> emissions must be reduced by a certain extent. Additionally, the study reveals that by reducing the fuel use, there would be a corresponding drop in the input exergy of the fuel. Consequently, this would enhance the exergy outputs and usable work produced by the Kalina cycle, water heat exchanger, and absorption chiller, so greatly optimizing the exergy efficiency. As a result, there would be minimal CO<sub>2</sub> emissions, and this improves the sustainability of the CCHP system.

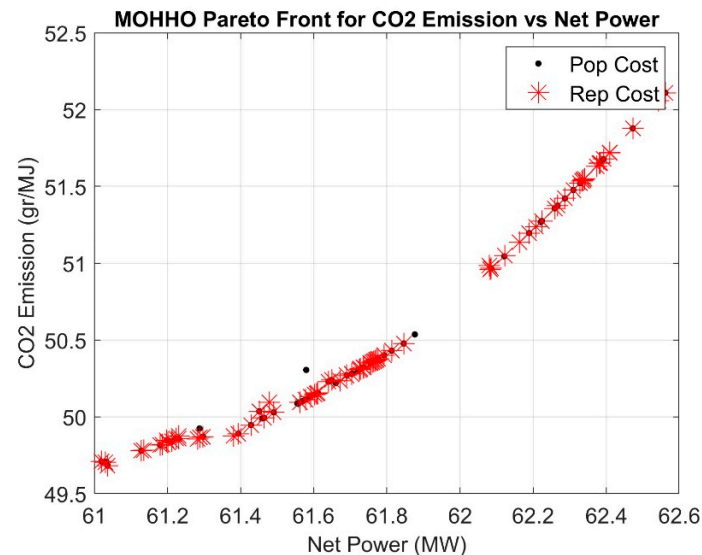


**Figure 5.** Pareto front showing the trade-off between CO<sub>2</sub> emissions and net power.

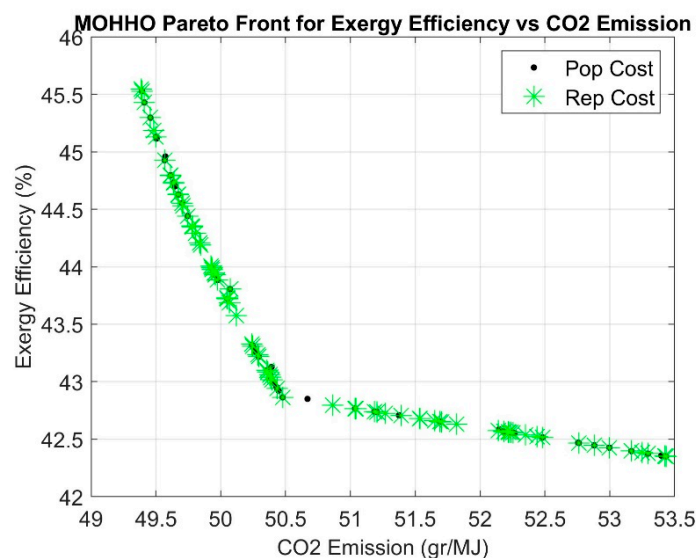


**Figure 6.** Pareto front showing the trade-off between exergy efficiency and CO<sub>2</sub> emissions.

Additionally, Figure 7 illustrates a negative correlation between the exergy efficiency and net power as increasing the net power from 61 to 62.75 MW which led to a 6% reduction in the exergy efficiency. This indicates that a system can have a high net power output yet still lack efficiency. This inverse relationship occurs because additional power output often relies on increased fuel combustion, which inherently has a lower exergy efficiency due to the waste heat and irreversibility in the combustion process. To address this effect, it is recommended to optimize the configuration of bottom cycle systems like the Kalina cycle and absorption chiller. Running these subsystems in a way that maximizes the use of waste

heat can improve the system’s overall exergy efficiency while reducing the fuel dependency. By focusing on non-combustible power sources such as the Kalina cycle, the system can achieve a cleaner energy output and improved efficiency without the drawbacks of high emissions and energy loss from additional fuel combustion.

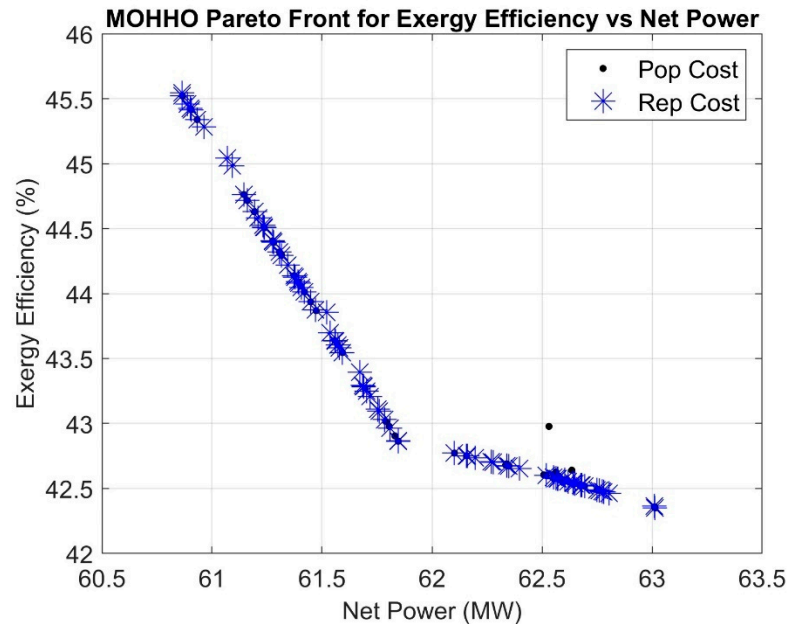


Figure 7. Pareto front showing the trade-off between exergy efficiency and net power.

The constraints placed on the HHO technique and the convergence of each choice variable are shown in Figure 8’s scatter plot distribution. The results show that lower compression ratios and pinch point temperatures are preferred by the suggested HHO strategy. However, values in the range between the minimum and the midpoint were selected, by the optimization method, for the combustion chamber inlet temperature. The scatter plot for the gas turbine inlet temperature is distributed between the constraint’s upper and lower bounds.

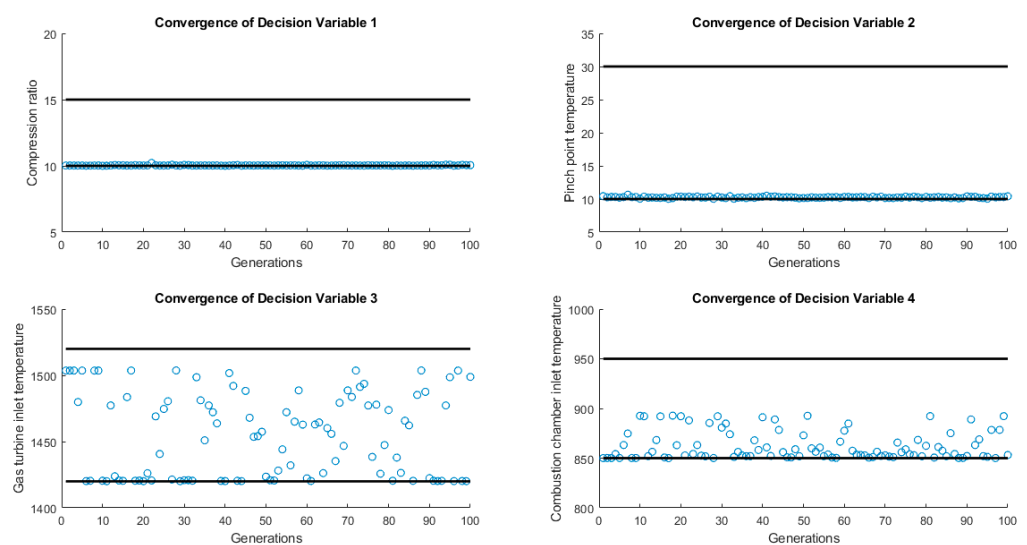


Figure 8. Scatter pattern of decision variables.

The MOHHO was designed to produce six ideal solutions, which were then compared with the outcomes of similar research that utilized the RSM. The data gathered, detailed

in Table 6, indicate that the MOHHO generally produced CO<sub>2</sub> emissions ranging from 50.33 gr/MJ to 50.66 gr/MJ, which is at least 4.2% lower than the CO<sub>2</sub> emission values produced by the RSM. The data in Table 6 yielded a high net power of 61.91 MW and low values of X<sub>1</sub>, X<sub>2</sub>, X<sub>3</sub>, and X<sub>4</sub>. This, however, resulted in high CO<sub>2</sub> emission and low exergy efficiency values. Better values of CO<sub>2</sub> emissions and exergy efficiency were obtained at relatively higher X<sub>3</sub> and X<sub>4</sub> values although at the reduced net power of 61.52 MW. Overall, the MOHHO yielded decision variable configurations that produced higher net power (61.91 MW), higher exergy efficiency (45.28%), and a relatively lower CO<sub>2</sub> emission (50.33 gr/MJ) as highlighted in Table 6. Therefore, the proposed MOHHO outperformed the RSM in optimizing the net power, CO<sub>2</sub> emission, and exergy efficiency.

**Table 6.** Comparison of optimization results with a related study.

Optimization Technique	Best-Performing Decision Variables				Optimal Performance Metrics		
	X <sub>1</sub>	X <sub>2</sub>	X <sub>3</sub>	X <sub>4</sub>	Net Power	CO <sub>2</sub> Emission	Exergy Efficiency
MOHHO	10	10	1420	855.34	61.91	50.61	42.84
	10	10	1422.67	850	61.82	50.44	42.94
	10.28	11.14	1514.57	896.17	61.52	50.66	45.28
	10	10	1426.26	850	61.78	50.38	43.04
	10.01	10.77	1469.76	870.77	61.60	50.33	44.15
	10.28	11.14	1514.31	896.01	61.52	50.66	45.28
RSM (Mahdavi, Mojaver, and Khalilarya [29])	11.66	11.96	1470	900	61.73	52.87	44.22
	11.11	20.00	1470	900	61.73	52.99	44.09
	11.98	20.00	1470	890	61.75	53.84	44.12
	12.50	16.10	1484	900	61.75	54.07	44.58
	12.50	15.72	1470	891	61.79	54.07	44.10
	12.50	20.00	1468	882	61.75	54.28	44.30

## 5. Conclusions

This study aimed to maximize the efficiency of a solar-assisted CCHP system through multi-objective optimization using the Harris Hawks approach. The optimization sought to minimize the greenhouse gas emissions, which have detrimental effects on human health and contribute to global warming while increasing the net power and energy efficiency. This study emphasizes how important it is to slow down the rate at which fossil fuels are depleting as demonstrated by the optimized solar-assisted CCHP system. In addition, this work introduces a new optimization strategy, whereas previous studies have utilized different methods to achieve the multi-objective optimization of the solar-powered CCHP system being studied. This method was employed due to its dynamic balance of various exploration and exploitation, its robustness across different kinds of objectives, and its fast convergence time. However, it had the drawback of premature convergence as seen with the inlet gas turbine temperature. The research's results and findings are described in the subsequent section.

- The most effective parameter configuration for the thermodynamic design of the solar-powered CCHP system is identified using a multi-objective optimization technique with decision variables including the compression ratio, pinch point temperature difference, turbine inlet temperature, and combustion chamber inlet temperature.
- The net power, CO<sub>2</sub> emissions, and exergy efficiency serve as objective functions for evaluating the efficacy of the CCHP system by assessing how effectively the decision variables meet the restrictions.

- The Harris Hawks technique is utilized to accomplish multi-objective optimization by generating non-dominated Pareto optimum solutions. This study calculates a collection of Pareto optimal solutions, which are then presented as alternative choices to the decision-maker. The objective is to empower the decision-makers to exercise their judgment and improve the efficiency of the CCHP system. The convergence of the individual decisions streamlines the decision-making process.
- Interestingly, the mutual reliance among the four decision variables, within the CCHP system under study, signifies that alterations to a single variable will invariably influence the remaining three. Consequently, employing a multi-objective optimization methodology is recommended for the comprehensive assessment of the system's operational efficacy.
- The research identified a conflict within the decision-making processes concerning the optimization of the net power and CO<sub>2</sub> emissions. Maximizing the net power tends to correlate with increased CO<sub>2</sub> emissions, presenting a trade-off as a higher net power often leads to elevated CO<sub>2</sub> emissions, which is undesirable.
- Another significant observation pertains to the correlation between exergy efficiency and CO<sub>2</sub> emissions. It suggests that a system characterized by minimal CO<sub>2</sub> emissions tends to exhibit high exergy efficiency. This indicates compatibility wherein a system with minimal CO<sub>2</sub> emissions tends to be highly efficient. The study's findings challenge the assumption that a system with high net power production invariably guarantees a high efficiency. This assertion is supported by the inverse relationship observed between the net power and exergy efficiency. Hence, it is important to note that attaining a high level of net power does not always result in a higher efficiency, as there exists a negative correlation between the net power and exergy efficiency.
- The analysis of the convergence of decision variables reveals that optimizing the objective values can be achieved by minimizing the compression ratio, pinch point temperature difference, and inlet combustion chamber temperature. However, it is noteworthy that the ranges for the gas turbine temperature are spread across the upper and lower bounds of the constraints. This dispersion suggests challenges in achieving convergence for this variable, hinting at the potential difficulties in its optimization. Consequently, additional techniques may be necessary to address these challenges and achieve convergence for the gas turbine temperature within the defined constraints. The HHO may be hybridized with the artificial neural network or the ant-lion approach to achieve optimal convergence. Also, adaptive tuning of the HHO parameters during the optimization process can be explored to improve the optimization performance.

As a recommendation, alternative meta-heuristic optimization techniques like genetic algorithms and particle swarm optimization could be explored to enhance the performance of the solar-assisted CCHP system. Additionally, predictive control methods, such as model predictive control and fuzzy logic control, can be combined with meta-heuristic solutions to dynamically adjust the CCHP system's configuration in response to changing environmental conditions and the preferences of users or decision-makers. Moreover, validating the optimal results obtained from these meta-heuristic approaches with experimental data would strengthen the credibility of the proposed solutions in practical applications. Finally, for future research, incorporating other renewable energy sources like wind and biomass, along with renewable energy storage systems, would significantly mitigate the variability in energy supply often encountered when relying solely on solar power.

**Supplementary Materials:** The following supporting information can be downloaded at: <https://www.mdpi.com/article/10.3390/su162310694/s1>.

**Author Contributions:** Conceptualization, U.U. and L.T.; methodology, formal analysis, writing—original draft preparation, U.U.; writing—review and editing, supervision, L.T. and C.W.L. All authors have read and agreed to the published version of the manuscript.

**Funding:** The APC was funded by the University of Johannesburg.

**Informed Consent Statement:** Not applicable.

**Data Availability Statement:** The original contributions presented in the study are included in the article/supplementary material, further inquiries can be directed to the corresponding author.

**Acknowledgments:** The authors wish to express their gratitude to the University of Johannesburg Research Committee and the Commonwealth Scholarship Fund for their support and sponsorship of this research.

**Conflicts of Interest:** The authors declare no conflicts of interest.

## Nomenclature

CCHP	Combined Cooling Heating and Power
CHP	Combined Heat and Power
GHG	Greenhouse Gas
HRSG	Heat Recovery Steam Generator
GT	Gas turbine
RSM	Response surface method
HHO	Harris Hawks Optimization
MOHHO	Multi-objective Harris Hawks Optimization
HTR	High Temperature Recuperator
LTR	Low Temperature Recuperator
SHE	Solution Heat Exchanger
APH	Air-preheater

## References

- Ramachandran, T.; Mourad, A.H.I.; Hamed, F. A Review on Solar Energy Utilization and Projects: Development in and around the UAE. *Energies* **2022**, *15*, 3754. [CrossRef]
- BP Energy Outlook. 2023. Available online: <https://www.bp.com/en/global/corporate/energy-economics/energy-outlook.html> (accessed on 31 May 2023).
- Ortiga, J.; Bruno, J.C.; Coronas, A. Operational optimization of a complex trigeneration system connected to a district heating and cooling network. *Appl. Therm. Eng.* **2013**, *50*, 1536–1542. [CrossRef]
- Lozano, M.A.; Carvalho, M.; Serra, L.M. Allocation of economic costs in trigeneration systems at variable load conditions. *Energy Build.* **2011**, *43*, 2869–2881. [CrossRef]
- Wang, L.; Lu, J.; Wang, W.; Ding, J. Energy, environmental and economic evaluation of the CCHP systems for a remote island in south of China. *Appl. Energy* **2016**, *183*, 874–883. [CrossRef]
- Sharma, M.K.; Bhattacharya, J. Finding optimal operating point for advection-cooled concentrated photovoltaic system. *Sustain. Energy Technol. Assess.* **2022**, *49*, 101769. [CrossRef]
- Dincer, I.; Zamfirescu, C. Renewable-energy-based multigeneration systems. *Int. J. Energy Res.* **2012**, *36*, 1403–1415. [CrossRef]
- Nadimi-Shahraki, M.H.; Taghian, S.; Mirjalili, S.; Zamani, H.; Bahreininejad, A. GGWO: Gaze cues learning-based grey wolf optimizer and its applications for solving engineering problems. *J. Comput. Sci.* **2022**, *61*, 101636. [CrossRef]
- Hansen, N.; Muller, S.D.; Koumoutsakos, P. Reducing the time complexity of the derandomized evolution strategy with covariance matrix adaptation (CMA-ES). *Evol. Comput.* **2003**, *11*, 1–18.
- Abualigah, L. Multi-verse optimizer algorithm: A comprehensive survey of its results, variants, and applications. *Neural Comput. Appl.* **2020**, *32*, 12381–12401. [CrossRef]
- Mirjalili, S.; Saremi, S.; Mirjalili, S.M.; Coelho, L.D.S. Multi-objective grey wolf optimizer: A novel algorithm for multi-criterion optimization. *Expert Syst. Appl.* **2016**, *47*, 106–119. [CrossRef]
- Hasanzadeh, R.; Mojaver, M.; Azdast, T.; Park, C.B. A novel systematic multi-objective optimization to achieve high-efficiency and low-emission waste polymeric foam gasification using response surface methodology and TOPSIS method. *Chem. Eng. J.* **2022**, *430*, 132958. [CrossRef]
- Ren, F.; Wang, J.; Zhu, S.; Chen, Y. Multi-objective optimization of combined cooling, heating and power system integrated with solar and geothermal energies. *Energy Convers. Manag.* **2019**, *197*, 111866. [CrossRef]
- Azaza, M.; Wallin, F. Multi objective particle swarm optimization of hybrid micro-grid system: A case study in Sweden. *Energy* **2017**, *123*, 108–118. [CrossRef]
- Shehab, M.; Mashal, I.; Momani, Z.; Shambour, M.K.Y.; Al-Badareen, A.; Al-Dabet, S.; Bataina, N.; Alsoud, A.R.; Abualigah, L. Harris Hawks Optimization Algorithm: Variants and Applications. *Arch. Comput. Methods Eng.* **2022**, *29*, 5579–5603. [CrossRef]

16. Sharifian, Y.; Abdi, H. Solving multi-zone combined heat and power economic emission dispatch problem considering wind uncertainty by applying grasshopper optimization algorithm. *Sustain. Energy Technol. Assess.* **2022**, *53*, 102512. [[CrossRef](#)]
17. Ji, J.; Wang, F.; Zhou, M.; Guo, R.; Ji, R.; Huang, H.; Zhang, J.; Nazir, M.S.; Peng, T.; Zhang, C.; et al. Evaluation Study on a Novel Structure CCHP System with a New Comprehensive Index Using Improved ALO Algorithm. *Sustainability* **2022**, *14*, 15419. [[CrossRef](#)]
18. Xu, L.; Luo, X.; Wen, Y.; Wu, T.; Wang, X.; Guan, X. Energy Management of Hybrid Power Ship System Using Adaptive Moth Flame Optimization Based on Multi-Populations. *IEEE Trans. Power Syst.* **2023**, *39*, 1711–1727. [[CrossRef](#)]
19. Ukaegbu, U.; Tartibu, L.; Lim, C.W. Multi-Objective Optimization of a Solar-Assisted Combined Cooling, Heating and Power Generation System Using the Greywolf Optimizer. *Algorithms* **2023**, *16*, 463. [[CrossRef](#)]
20. Wang, J.; Han, Z.; Guan, Z. Hybrid solar-assisted combined cooling, heating, and power systems: A review. *Renew. Sustain. Energy Rev.* **2020**, *133*, 110256. [[CrossRef](#)]
21. Cao, Y.; Dhahad, H.A.; Togun, H.; Haghghi, M.A.; Athari, H.; Mohamed, A.M. Exergetic and economic assessments and multi-objective optimization of a modified solar-powered CCHP system with thermal energy storage. *J. Build. Eng.* **2021**, *43*, 102702. [[CrossRef](#)]
22. Wang, J.; Lu, Y.; Yang, Y.; Mao, T. Thermodynamic performance analysis and optimization of a solar-assisted combined cooling, heating and power system. *Energy* **2016**, *115*, 49–59. [[CrossRef](#)]
23. Wang, J.; Liu, Y.; Ren, F.; Lu, S. Multi-objective optimization and selection of hybrid combined cooling, heating and power systems considering operational flexibility. *Energy* **2020**, *197*, 117313. [[CrossRef](#)]
24. Song, Z.; Liu, T.; Lin, Q. Multi-objective optimization of a solar hybrid CCHP system based on different operation modes. *Energy* **2020**, *206*, 118125. [[CrossRef](#)]
25. Abba, S.I.; Rotimi, A.; Musa, B.; Yimen, N.; Kawu, S.J.; Lawan, S.M.; Dagbasi, M. Emerging Harris Hawks Optimization based load demand forecasting and optimal sizing of stand-alone hybrid renewable energy systems—A case study of Kano and Abuja, Nigeria. *Results Eng.* **2021**, *12*, 100260. [[CrossRef](#)]
26. Yousri, D.; Babu, T.S.; Fathy, A. Recent methodology based Harris Hawks optimizer for designing load frequency control incorporated in multi-interconnected renewable energy plants. *Sustain. Energy Grids Netw.* **2020**, *22*, 100352. [[CrossRef](#)]
27. Zhao, L.; Li, Z.; Chen, H.; Li, J.; Xiao, J.; Yousefi, N. A multi-criteria optimization for a CCHP with the fuel cell as primary mover using modified Harris Hawks optimization. *Energy Sources Part A Recovery Util. Environ. Eff.* **2020**, *46*, 10630–10645. [[CrossRef](#)]
28. Song, Y.; Tan, X.; Mizzi, S. Optimal parameter extraction of the proton exchange membrane fuel cells based on a new Harris Hawks Optimization algorithm. *Energy Sources Part Recovery Util. Environ. Eff.* **2020**, *46*, 8718–8735. [[CrossRef](#)]
29. Pandey, A.K.; Jadoun, V.K. Real-time and day-ahead risk averse multi-objective operational scheduling of virtual power plant using modified Harris Hawk's optimization. *Electr. Power Syst. Res.* **2023**, *220*, 109285. [[CrossRef](#)]
30. Mahalekshmi, T.; Maruthupandi, P. Multiobjective Economic/Environmental Dispatch Using Harris Hawks Optimization Algorithm. *Intell. Autom. Soft Comput.* **2023**, *36*, 445–460. [[CrossRef](#)]
31. Mahdavi, N.; Mojaver, P.; Khalilarya, S. Multi-objective optimization of power, CO<sub>2</sub> emission and exergy efficiency of a novel solar-assisted CCHP system using RSM and TOPSIS coupled method. *Renew. Energy* **2022**, *185*, 506–524. [[CrossRef](#)]
32. Costa, E.; Almeida, M.F.; Alvim-Ferraz, C.; Dias, J.M. Otimization of Crambe abyssinica enzymatic transesterification using response surface methodology. *Renew. Energy* **2021**, *174*, 444–452. [[CrossRef](#)]
33. Kumar, R. A critical review on energy, exergy, exergoeconomic and economic (4-E) analysis of thermal power plants. *Eng. Sci. Technol. Int. J.* **2017**, *20*, 283–292. [[CrossRef](#)]
34. Bednarz, J.C. Cooperative hunting Harris' hawks (*Parabuteo unicinctus*). *Science* **1988**, *239*, 1525–1527. [[CrossRef](#)] [[PubMed](#)]
35. Heidari, A.A.; Mirjalili, S.; Faris, H.; Aljarah, I.; Mafarja, M.; Chen, H. Harris hawks optimization: Algorithm and applications. *Future Gener. Comput. Syst.* **2019**, *97*, 849–872. [[CrossRef](#)]
36. Mousafarash, A. Exergy and Exergoenvironmental Analysis of a CCHP System Based on a Parallel Flow Double-Effect Absorption Chiller. *Int. J. Chem. Eng.* **2016**, *1*, 2370305. [[CrossRef](#)]
37. Zhang, D.; Yang, X.; Li, H.; Jia, Z.; Zhang, S.; Tang, S.; Liu, D.; Wu, X. 4E analysis and parameter study of a solar-thermochemical energy storage CCHP system. *Energy Convers. Manag.* **2024**, *301*, 118002. [[CrossRef](#)]

**Disclaimer/Publisher's Note:** The statements, opinions and data contained in all publications are solely those of the individual author(s) and contributor(s) and not of MDPI and/or the editor(s). MDPI and/or the editor(s) disclaim responsibility for any injury to people or property resulting from any ideas, methods, instructions or products referred to in the content.